

## Near surface mounted CFRP-based technique for the strengthening of concrete structures

Joaquim Barros, José Sena-Cruz, Salvador Dias, Débora Ferreira, Adriano Fortes

University of Minho

Department of Civil Engineering

Campus de Azurém, 4800-058 Guimarães Portugal

**Abstract:** To assess the effectiveness of the Near Surface Mounted (NSM) strengthening technique, an experimental program was carried out involving reinforced concrete (RC) columns and beams. In columns failing in bending the present work shows that the failure strain of the Carbon Fiber Reinforced Polymer (CFRP) laminates can be attained using the NSM technique. Beams failing in bending were also strengthened with CFRP laminates in order to double their load carrying capacity. This goal was attained and maximum strain levels of about 90% of the CFRP failure strain were recorded. Performance of externally bonded reinforcing (EBR) and NMS techniques was compared for strengthening RC beams failing in shear. NMS was much more effective, not only in terms of the increase of the load carrying capacity and deformability at beam failure, but also with respect to the time consuming nature of the corresponding strengthening procedures. To assess the bond behavior of CFRP to concrete, pullout-bending tests were carried out. The influences of bond length and concrete strength on the bond behavior were analyzed.

**Keywords:** Carbon Fiber Reinforced Polymers, Strengthening, Concrete, Columns, Beams, Flexural, Shear, Bond

### 1. Introduction

The use of fiber reinforced polymer (FRP) materials for structural repair and strengthening has continuously increased during previous years, due to several advantages associated with these composites when compared to conventional materials like steel. These benefits include low weight, easy installation, high durability and tensile strength, electromagnetic neutrality and practically unlimited availability in size, geometry and dimension [1, 2].

FRP laminates and sheets are generally applied on the faces of the elements to be strengthened, using externally bonded reinforcing (EBR) technique. The research carried out up to now has revealed that this technique cannot mobilize the full tensile strength of FRP materials due to premature debonding [3, 4]. Since FRP systems are directly exposed to weathering conditions, negative influences of freeze/thaw cycles [5] and the effect of high and low temperatures [6] should be taken into account in the reinforcing performance of these materials. In

addition, EBR systems are susceptible to fire and acts of vandalism.

In an attempt at overcoming these drawbacks, a recent strengthening technique designated by near surface mounted (NSM) has been proposed, where FRP rods are fixed into pre-cut grooves on the concrete cover of the elements to be strengthened [7]. This technique has been used in some practical applications [8, 9, 10] and several benefits have been pointed out.

Blaschko and Zilch [11] proposed a similar strengthening technique based on introducing laminate strips of CFRP into pre-cut slits on the concrete cover. The CFRP was bonded to concrete by epoxy adhesive. Despite the few number of carried out tests, the obtained results revealed this to be a promising technique.

In recent years, carbon and glass FRP sheets have been applied using the retrofitting technique to increase concrete confinement [12, 13] and bending resistance [14] of reinforced concrete (RC) columns. This increase is dependent on the thickness (number of layers) and on the material properties of the FRP system [13, 15], as well as on column cross-sectional geometry [16]. Blaschko and Zilch [11] showed that the bending resistance of concrete elements can be significantly increased using laminate strips bonded to concrete into slits. The effectiveness of this strengthening technique, however, has not yet been appraised in concrete columns failing in bending and simultaneously submitted a kind of seismic loading configuration (lateral cyclic loading and static axial compression load). One of the goals of the present work is to assess the benefits of this strengthening technique on this type of structural elements.

EBR techniques using CFRP materials have also been used to increase the shear resistance of RC beams [17, 18, 19]. Premature failures of these CFRP systems, however, inhibited the attainment of the desired strengthening efficacy level. In an attempt at obtaining a more effective shear strengthening technique for concrete beams, De Lorenzis *et al.* [20] used CFRP rods introduced into grooves made onto the vertical faces of concrete beams. This strengthening technique provided a significant increase on the shear resistance of the strengthened beams. Following similar strengthening technique

procedures, but using laminate strips of CFRP bonded to concrete into thin slits, the effectiveness of this technique for shear strengthening is also assessed in the present work.

Since bond behavior analysis is a requirement for understanding the stress transfer process between concrete and CFRP, the present work conducts a pullout-bending test similar to the one proposed by RILEM for assessing the bond characteristics of conventional steel rods [21]. Using the same slit size and epoxy adhesive, bond behavior was analyzed in order to determine the influences of both bond length and concrete strength.

## 2. Experimental program and strengthening technique

Table I summarizes the experimental program and its main objectives. It includes a group of series of tests with RC columns and RC beams, all failing in bending, a group of series of tests with RC beams failing in shear, and a group of series of pullout-bending tests. The first two groups have the main purpose of assessing the effectiveness of the NSM technique on elements failing in bending and on elements failing in shear, respectively. The percentage of the steel reinforcement ratio,  $\rho_{sl}$  (ratio between the cross sectional area of longitudinal steel bars and the cross sectional area of the concrete element), has a recognized influence on the effectiveness of FRP strengthening techniques. To assess this influence on the NSM technique applied to RC elements failing in bending, tests with columns and beams of distinct  $\rho_{sl}$  were carried out. The effectiveness of EBS and NSM techniques were compared in the series of RC beams failing in shear.

Elements failing in bending		Elements failing in shear
RC columns	RC beams	
Cyclic tests	Monotonic tests	
Cyclic horizontal increasing load and static axial load	Four point bending tests	
Assess the influence of the longitudinal steel reinforcement ratio, $\rho_{sl}$	Compare the performance of EBR and NSM techniques	
Two distinct $\rho_{sl}$	Four distinct $\rho_{sl}$	Strips of wet lay-up CFRP; CFRP laminates embedded into slits
<b>Pullout-bending tests</b>		
Concrete beams		
Monotonic tests		
Four point bending tests		
Asses the bond behavior of CFRP concrete		
Bond Length and concrete strength		

Table I : Experimental program

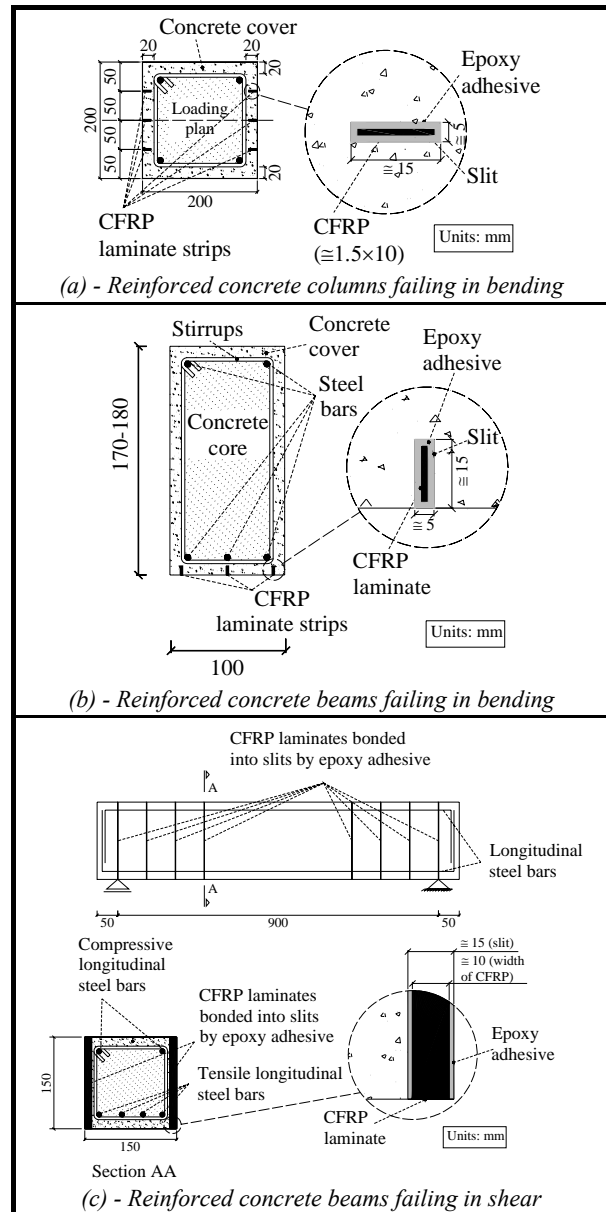


Fig. 1 : NSM CFRP Technique

The strengthening technique is made up of the following steps (see Figure 1):

- Using a diamond cutter, slits of 4 to 5 mm width and 12 to 15 mm depth are executed on the concrete surface of the elements to be strengthened;
- Slits are cleaned by compressed air;
- Laminate strips of CFRP are cleaned by acetone;
- Epoxy adhesive is produced according to supplier recommendations;
- Slits are filled with the epoxy adhesive;
- The epoxy adhesive is applied on the faces of the laminate strips of CFRP;
- Laminate strips of CFRP are introduced into the slits and the epoxy adhesive in excess is removed.

The curing/hardening process of the epoxy adhesive lasted for, at least, five days prior to testing the strengthened elements.

### 3. Materials properties

#### 3.1. Concrete and steel bars

Table II includes the main properties of the concrete and steel bars used in the experimental program. The concrete compression strength,  $f_{cm}$ , was obtained from uniaxial compression tests with cylinder specimens of 150 mm diameter and 300 mm height. The concrete tensile flexural strength,  $f_{ctm,fl}$ , and the concrete fracture energy,  $G_f$ , were obtained from three point bending tests with notched beams, performed according to the recommendations of RILEM [22]. Each value was the average result of, at least, three tests. In the series of RC columns, low strength concrete and steel bars of moderate strength and smooth surface were used to obtain representative specimens of concrete columns of Portuguese buildings built before the 1980s.

Steel bars were tested according to the standard EN 10 002-1 [23], and each result was the average of at least five tests.

#### 3.2. CFRP and epoxy adhesive

According to the supplier, the MBrace Sheet C5-30 used as shear reinforcement in beams failing in shear, has the properties indicated in Table III. Laminate strips of CFRP used in the NSM technique, with the designation of CFK 150/2000 10x1.4, were delivered in rolls and had cross sectional dimensions of  $9.59 \pm 0.09$  mm width and  $1.45 \pm 0.005$  mm thickness (average values of fifteen measures). From three uniaxial tensile tests carried out according to ISO 527-5 standard [24], it was verified that the tensile behavior of the CFRP roll delivered for the concrete column series of tests was distinct from the tensile behavior registered in the rolls delivered for the beam series of tests, see Table III [25, 26]. This table also includes the Young's modulus and the tensile strength range of the epoxy adhesive used in the NSM technique, obtained from five uniaxial tensile tests carried out according to ISO 527-3 standard [27].

#### 3.3. Epoxy mortar

To anchor the laminate strips of CFRP to the column foundation in the RC column test series, an epoxy mortar was used (see Figure 2). This epoxy mortar was composed of one part epoxy and three parts of previously washed and dried fine sand (parts measured in weight). Following the European standard EN 196-1 [28], an average compressive

strength of  $51.7 \text{ N/mm}^2$  and an average flexural tensile strength of  $35.4 \text{ N/mm}^2$  was obtained at 28 days [29].

Element type		Concrete			Steel		
		$f_{cm}$ [MPa]	$f_{ctm,fl}$ [MPa]	$G_f$ [N/mm]	$\phi_s$ [mm]	$f_{sy}$ [MPa]	$f_{su}$ [MPa]
Elements failing in bending	RC columns	16.7 (28) <sup>1</sup>	2.62 (28)	0.08 (28)	6	352.4	532.8
					10	323.3	456.5
					12	364.8	518.8
	RC beams	46.1 (90)	-	-	6	-	750
					8	-	500
Elements failing in shear	RC beams	49.5 (28) 56.2 (105)	-	-	(stirrups) 6	540	694
					(long.) 6	618	691
					10	464	581
Pullout bending tests	Concrete beams	34.9	5.9	-	-	-	-

1 - The values in brackets represent the age, in days, when the tests were carried out.

Table II : Properties of the concrete and steel bars

CFRP system		Main properties			
Type	Material	Tensile strength (MPa)	Young's modulus (GPa)	Ultimate strain (%)	Thickness (mm)
MBrace Sheet C5-30 <sup>1</sup>	Primer	12	0.7	3.0	-
	Epoxy	54	3	2.5	-
	Sheet	3000	390	0.8	0.167
CFK 150/2000 10x1.4 <sup>2</sup>	Adhesive	16-22	5	-	-
	Laminate	(i) 1741	153	1.1	9.6
		(ii) 2740	158	1.7	
		(iii) 2286	166	1.3	

<sup>1</sup> According to the supplier; <sup>2</sup> Evaluated from experimental tests  
(i) Columns; (ii) Beams failing in bending and pullout-bending tests; (iii) Beams failing in shear

Table III : Properties of the CFRP materials

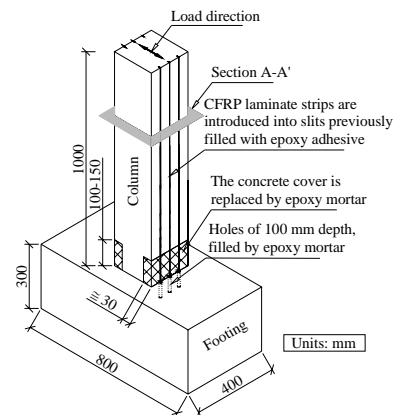


Fig. 2 : Strengthening technique in specimens of RC column (Section A-A' in Figure 1a)

## 4. Concrete columns failing in bending

### 4.1. Series of tests

Columns of reinforced concrete framed structures are the most vulnerable elements since their failure leads to the collapse of the structure. To assess the effectiveness of the NSM strengthening technique for concrete columns submitted to static axial compression load and cyclic horizontal increasing load, the three series of reinforced concrete columns, indicated in Table IV, were tested. Series NON consisted of non-strengthened columns, series PRE was composed of concrete columns strengthened with CFRP laminate strips before testing, and series POS consisted of previously tested columns of series NON which were post-strengthened with CFRP. The designation  $Pnm\_s$  was attributed to tests of series  $s$  (NON, PRE or POS), where  $n$  represents the diameter of the longitudinal steel bars, in mm, (10 or 12), and  $m$  can be  $a$  or  $b$ , since there are two specimens for each series of distinct longitudinal steel reinforcement ratio.

Longitudinal steel reinforcement	Series		
	NON <sup>1</sup>	PRE <sup>2</sup>	POS <sup>3</sup>
4 $\phi$ 10 ( $A_{st} = 314 \text{ mm}^2$ )	P10a_NON	P10a_PRE	P10a_POS
	P10b_NON	P10b_PRE	P10b_POS
4 $\phi$ 12 ( $A_{st} = 452 \text{ mm}^2$ )	P12a_NON	P12a_PRE	P12a_POS
	P12b_NON	P12b_PRE	P12b_POS

<sup>1</sup> Non-strengthened; <sup>2</sup> Strengthened before testing;

<sup>3</sup> Columns of NON series after have been tested and strengthened.

Table IV : Denominations for the RC column specimens

### 4.2. Test set-up and procedure

The test set-up is illustrated in Figure 3, where it can be seen that each specimen is composed of a column monolithically connected to a footing fixed to a foundation block by four steel bars. A constant vertical load of approximately 150 kN was applied to the column, inducing an axial compression stress of  $3.75 \text{ N/mm}^2$ . Linear variable displacement transducers (LVDTs) were used to record the horizontal displacements of the column as well as any vertical movement of the footing, see Figure 4. The position of the strain-gauges (SG) glued on the CFRP is also indicated in this figure. The tests were carried out with closed loop servo-controlled equipment. A history of displacements was imposed for LVDT1, located at the same height as the horizontal actuator, see Figures 3 and 4. The history of horizontal displacements included eight load cycles between  $\pm 2.5 \text{ mm}$  and  $\pm 20.0 \text{ mm}$ , in increments of  $\pm 2.5 \text{ mm}$ , with a displacement rate of  $150 \mu\text{m/s}$  [29].

### 4.3. Specific strengthening procedures

Figure 2 illustrates the strengthening technique adopted for the concrete columns. To anchor the CFRP laminate strips to the footing and to maintain their vertical position, the concrete cover of a region having a height of 100 to 150 mm from the bottom of the column (denoted here by “non-linear hinge region”) was removed. Afterwards, slits were executed along the faces subjected to tensile stress. In the alignment of the slits, perforations of about 100 mm depth were made in the footing to anchor the CFRP laminate strips. The slits and the holes were cleaned using steel brushes and compressed air. After filling the grooves with the epoxy adhesive, laminate strips of CFRP were inserted into the slits and the “non-linear hinge region” and the holes in the footing were filled with epoxy mortar. A more detailed description of the strengthening technique is provided elsewhere [29].

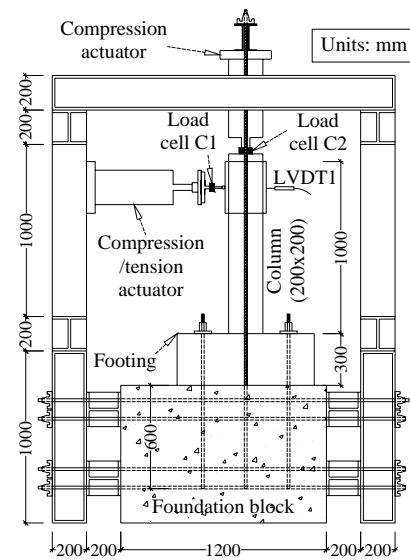


Fig. 3 : Test set-up (dimensions in mm)

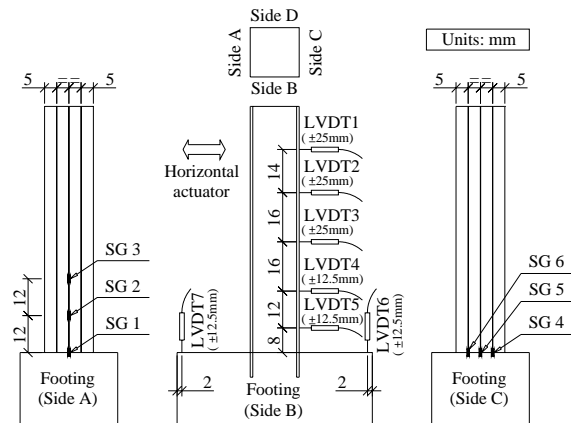


Fig. 4 : Location of the displacement transducers (LVDT) and strain gauges (SG) in test set-up

#### 4.4. Results

Representative results are presented in this section. Detailed results and analysis can be found elsewhere [30].

##### 4.4.1 Load carrying capacity

The maximum compressive and tensile forces obtained in the tests are given in Tables V and VI.

Force	Series PRE			
	P10a_PRE (111)	P10b_PRE (113)	P12a_PRE (110)	P12b_PRE (115)
Tensile [kN]	37.14	40.63	44.13	39.81
Compressive [kN]	-38.54	-37.96	-43.66	-36.64

Note: Values inside parenthesis indicate the age of the columns at testing, in days.

Table V : Maximum forces obtained in the columns of series PRE

Force	Series	P10a_	P10b_	P12a_	P12b_
Tensile	NON [kN]	16.67 (86)	21.78 (85)	26.35 (85)	29.31 (85)
	POS [kN]	37.96 (146)	41.38 (130)	34.11 (150)	45.54 (154)
	Increase [%]	127.70	89.99	29.45	55.37
Compressive	NON [kN]	-19.76 (86)	-24.07 (85)	-30.52 (85)	-32.27 (85)
	POS [kN]	-34.11 (146)	-43.1 (130)	-37.03 (150)	-41.58 (154)
	Increase [%]	72.62	79.06	21.33	28.85

Note: Values inside parenthesis indicate the age of the columns at testing, in days.

Table VI : Maximum forces obtained in the columns of NON and POS series

The differences recorded in the maximum forces of the columns from the same series were due to the compression strength variability of the concrete of these columns (two batches were required to build a specimen), as well as differences in the positioning of the steel bars and their properties. Taking into account the results obtained from the non-strengthened columns (series NON), a significant increase in the maximum load of the columns of series PRE (strengthened before testing) and POS (strengthened after NON series had been tested) was observed. The comparison between series NON and PRE should be made with caution, because the concrete compression strength of the columns of these two series was not the same. As the CFRP reinforcement ratio was the same for all the column specimens tested, the increase of the ultimate load was larger in columns of a lower steel reinforcement ratio. The increase of the load carrying capacity in PRE and POS series was similar.

##### 4.4.2 Force-deflection relationship

Figure 5 depicts a typical relationship between the horizontal force and the deflection at LVDT1 (see Figure 3). Since this strengthening technique does not provide significant concrete confinement, the increase on the dissipated energy was marginal.

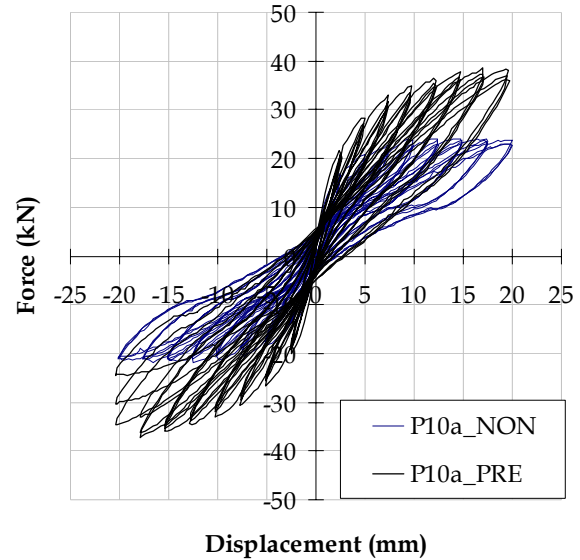


Fig. 5 : Cyclic force-deflection (at LVDT1) relationship for column P10a

The increment on the load carrying capacity, however, was significant as can be seen in Figure 6, where a typical envelope of the maximum values of the relationship between the maximum force registered in the load cycles and its corresponding deflection in the LVDT1 is represented.

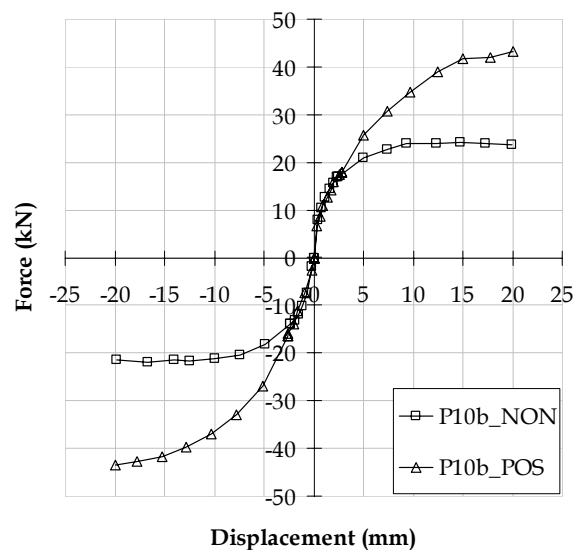


Fig. 6 : Force-deflection (at LVDT1) envelope of all load cycles for column P10b

#### 4.4.3 Force-Strain relationship

In the majority of the strengthened columns some laminate strips of CFRP reached tensile strain values close to the ultimate rupture strain of the CFRP ( $\approx 1.0\%$ ). Some CFRP laminate strips even failed at the main fracture surface of the concrete column. As an example, Figure 7 illustrates the relationship between the horizontal force applied to the column and the strain in the strain-gauge SG6, for the column P10a\_POS. In strain-gauges located at the concrete failure region, similar relationships to that depicted in Figure 7 were obtained in the remaining columns.

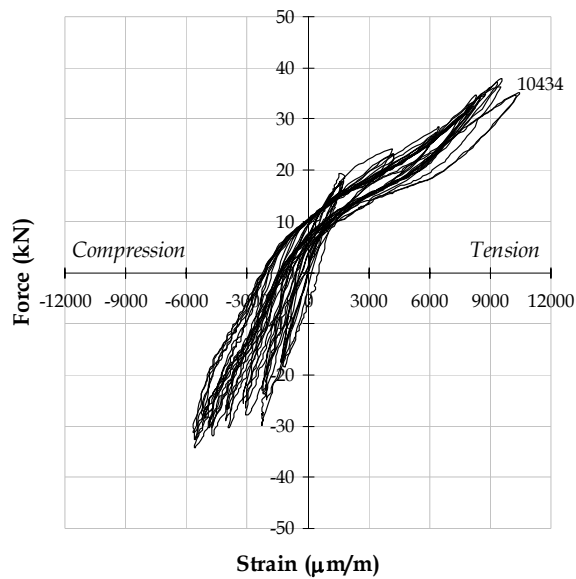
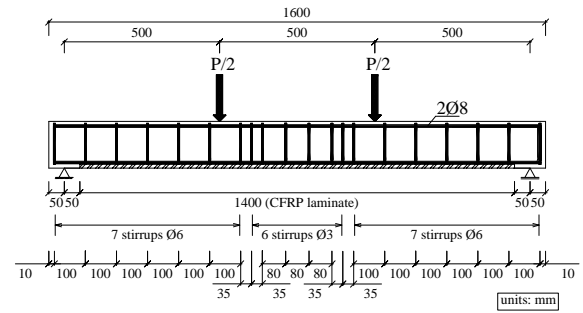


Fig. 7 : Relationship between the force and the strain on the strain gauge SG6 (see Figure 4) for the column P10a\_POS

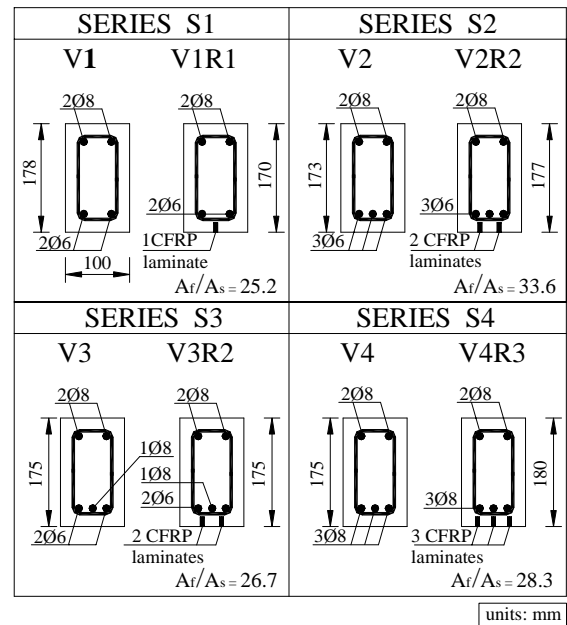
## 5. Concrete beams failing in bending

### 5.1. Series of beams

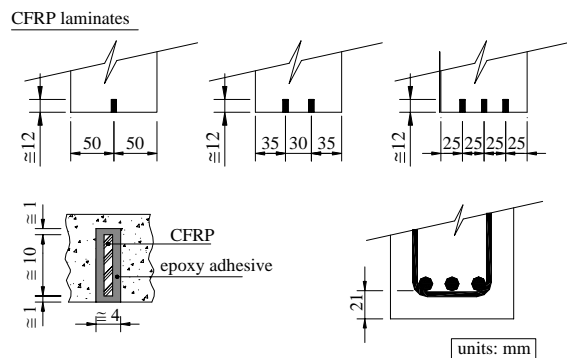
Figure 8 represents the geometry of the beams, the reinforcement arrangement and the number and position of the laminate strips of CFRP. The load configuration and the support conditions are also schematized. The cross sectional area of the CFRP,  $A_f$ , applied in the beam of each series, was designed to achieve twice the ultimate load of the corresponding reference beam. Shear reinforcement was selected to assure bending failure prior to shear failure for all beams. The cross sectional area of the tensile longitudinal steel bars is also indicated in Figure 8,  $A_s$ . The longitudinal steel reinforcement was composed of bars of 6 mm and 8 mm diameters, while stirrups were made of bars of 6 mm diameter. The beams were tested at the age of about 90 days.



a)



b)



c)

Fig. 8 : Series of beams failing in bending: (a) load configuration and arrangement of longitudinal reinforcement, (b) cross section of series of beams, (c) strengthening details

### 5.2. Test configuration and measuring devices

To evaluate the strain evolution of the CFRP laminate strips, strain gauges were glued on one of their lateral faces, according to the scheme shown in Figure 9. This figure also represents the position of

the LVDTs used for measuring the deflections of the beams.

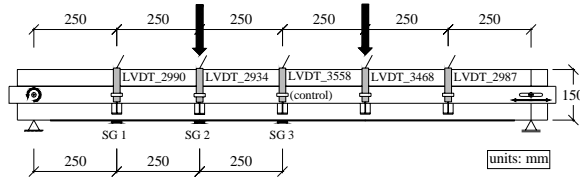


Fig. 9 : Measuring devices (LVDT - Linear Variable Displacement Transducer; SG - Strain Gauge)

### 5.3. Results

The failure modes and the interpretation of the reinforcing mechanisms provided by laminate strips of CFRP have been presented elsewhere [30].

#### 5.3.1 Force-Deflection relationship

The force-deflection relationships for the series of tested beams are depicted in Figure 10, and the main results are presented in Table VII. It is observed that the purpose of doubling the ultimate load ( $F_{max}$ ) of the corresponding reference beam was practically achieved. The increase on the load at the onset of yielding the steel reinforcement ( $F_{sy}$  - yielding load) was also significant, varying from 32% to 47%. The displacement corresponding to  $F_{sy}$  increased, as well as the cracking load,  $F_{cr}$ , and the serviceability load,  $F_{serv}$ , (the load for a deflection of  $L/400=3.75$  mm, where  $L$  is the beam span). A maximum increase of 45% and 47% on  $F_{serv}$  and  $F_{sy}$ , respectively, was recorded.

Series	Beam	$F_{cr}$ [kN]	$F_{serv}$ [kN]	$F_{sy}$ [kN]	$F_{max}$ [kN]	$\epsilon_{f,max}$ (%)
S1	V1	8.5	18.6	24.5	28.2	
	V1R1	10.7	22.7	32.31	50.3 <sup>(1)</sup>	1.55
S2	V2	8.1	21.7	37.5	41.0	
	V2R2	12.3	31.4	52.28	78.5	1.28
S3	V3	7.9	23.8	40.0	41.3	
	V3R2	11.9	32.8	54.52	81.9	1.28
S4	V4	8.1	32.3	46.9	48.5	
	V4R3	14.1	40.4	69.11	94.9	1.06

<sup>(1)</sup> The test was canceled at a load of 50.3 kN, when the deflection at mid-span was greater than 25mm.

Table VII : Main results obtained in the series of beams failing in bending

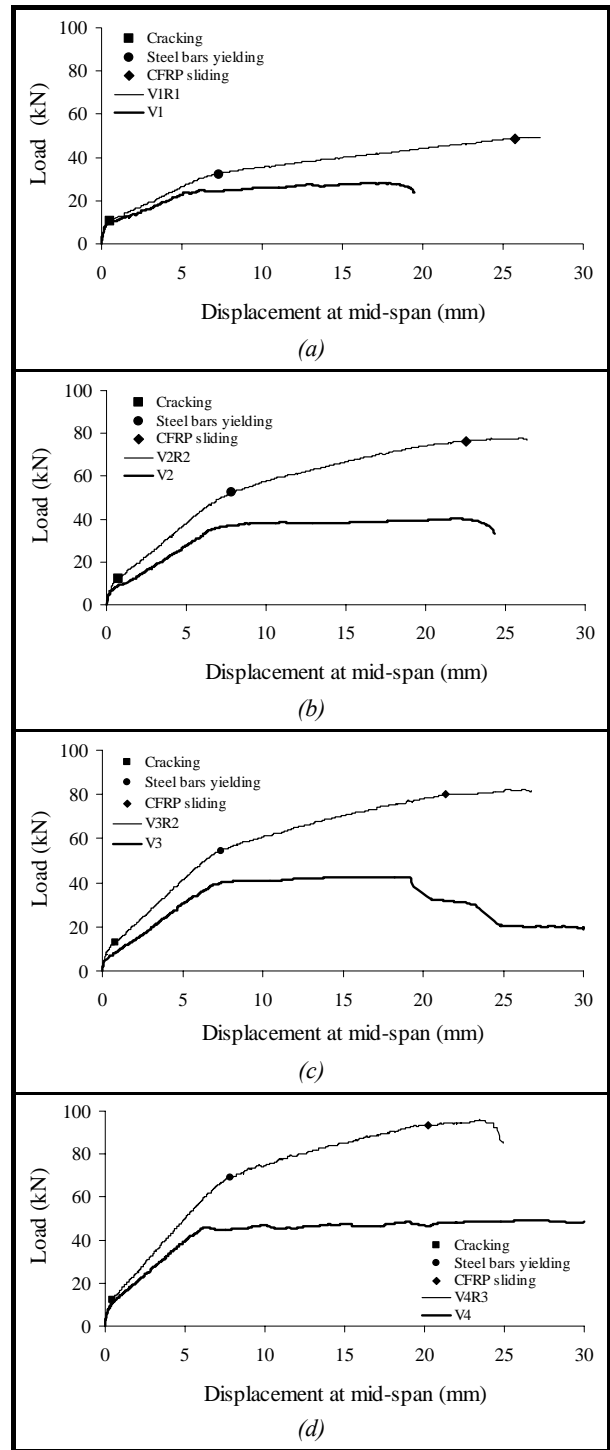


Fig. 10 : Force-deflection relationships of series: (a) S1, (b) S2, (c) S3 and (d) S4

#### 5.3.2 Force-Strain relationship

The relationships between the applied load and the strains recorded in the strain gauges glued onto the laminate strips of CFRP (see Figure 9) are depicted in Figure 11. The maximum strains obtained from the strengthened beams, and presented in

Table VII ( $\varepsilon_{f,max}$ ), ranged from 62% to 91% of the CFRP ultimate rupture strain ( $\varepsilon_{fu} \cong 1.7\%$ ), showing this strengthening technique has high level of effectiveness.

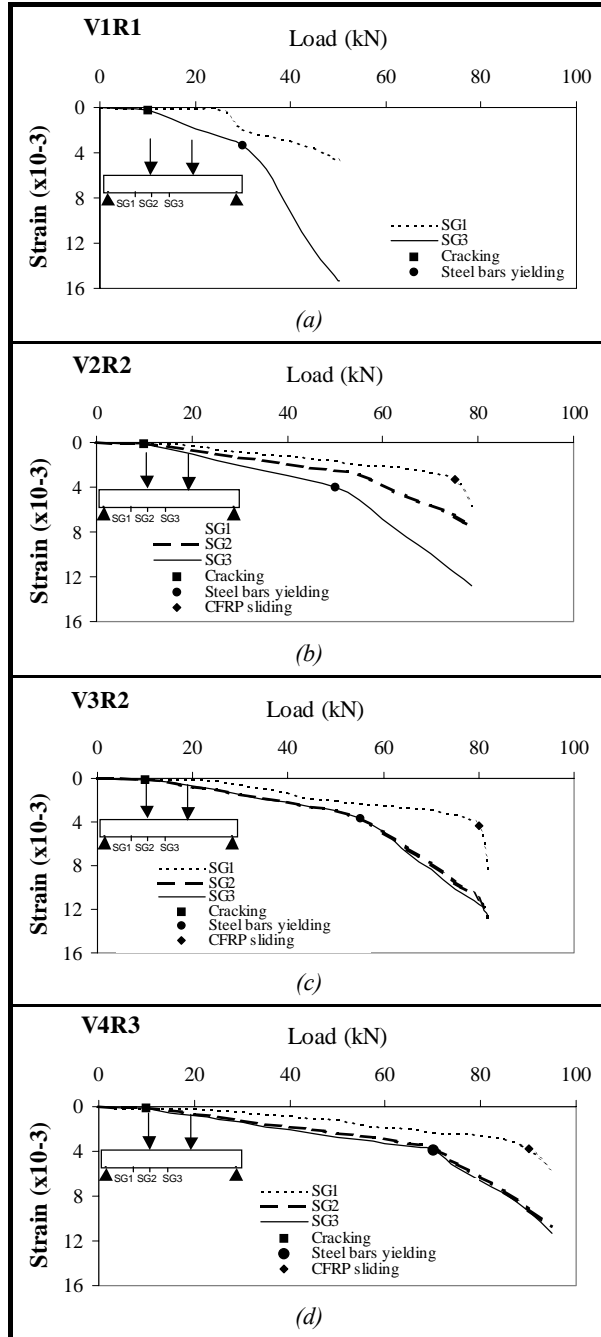


Fig. 11 : Force-strain relationships of series: (a) V1R1, (b) V2R2, (c) V3R2 and (d) V4R3

## 6. Concrete beams failing in shear

### 6.1. Series of tests

Three types of strengthening techniques using CFRP materials were applied to evaluate the most effective one for shear strengthening of RC beams. The series of beams tested (see Figure 12) contain a reference beam without any shear reinforcement (VB10); a beam with steel stirrups of 6 mm diameter spaced at 150 mm in the shear spans (VBE-15); a beam with strips of CFRP MBrace C5-30 sheet (properties in Table III) of two layers of 25 mm width and spaced at 80 mm in the shear spans (VBM-8); a beam with vertical laminate strips of CFRP bonded into pre-cut slits on the concrete cover of the vertical faces of the beam (see Figure 1c) and spaced at 100 mm (VBCV-10); and a beam with inclined (45 degrees) laminate strips of CFRP fixed onto the beam like the previous one (VBCI-15). The strips of the CFRP sheet in VBM-8 beam had a “U” shape (embracing the bottom and vertical faces of the beam). The amount of shear reinforcement applied in the beams was designed to provide similar shear resistance [1] and to assure that they would fail in shear mode. The beams were tested at the age of 105 days.

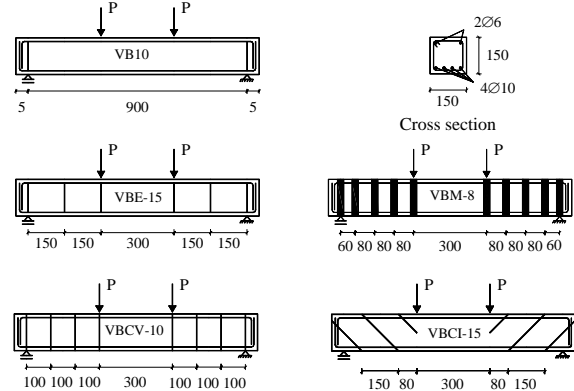


Fig. 12 : Series of beams failing in shear (unities: mm)

### 6.2. Results

Figure 13 represents the relationship between the load and the displacement at mid span of the tested beams. The main results are presented in Table VIII. When compared to the reference beam (VB10), the beams strengthened with CFRP materials attained an increase in the maximum load,  $F_{max}$ , ranging from 50% to 77%. The highest and the lowest increase of  $F_{max}$  occurred in the beam strengthened with vertical laminate strips of CFRP (VBCV-10) and in the beam strengthened with strips of CFRP sheet (VBM-8). The lowest effectiveness of the EBR technique (in the VBM-8 beam) can be justified by the failure modes of the strengthened beams. In VBM-8 beam a very fragile rupture occurred after the formation of the failure shear crack. The strips of CFRP sheet crossing the failure shear crack were ruptured at beam edges.

Delamination between these strips of CFRP and concrete was also observed. The failure mode of the beams VBCV-10 and VBCI-15 was not as fragile as the failure mode of VBM-8 beam. For deflections larger than the deflection corresponding to peak load, the beams reinforced with laminate strips of CFRP sustained appreciable residual force, which was not the case of beam VBM-8. When compared to the beam reinforced with steel stirrups (VBE-15), the beam strengthened with vertical laminate strips of CFRP had an increase of 9% in the maximum load. When compared to the deflection at maximum load of the reference beam ( $\delta_{p,VB10}$ ), the deflection at maximum load of beams VBE-15, VBCV-10, VBCI-15 and VBM-8 was 294%, 232%, 119% and 118% larger. Therefore,  $\delta_{p,VBCV-10}$  was 84% of  $\delta_{p,VBE-15}$ , showing that this strengthening technique was not only effective in terms of increasing the ultimate load, but also in assuring a high level of deformability at beam failure.

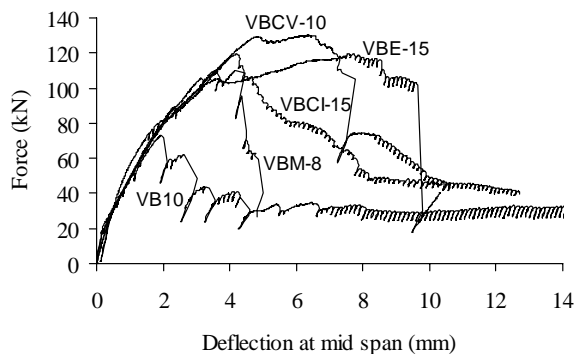


Fig. 13 : Relationship between the force and the deflection at mid span of the beams failing in shear

Beam	$F_{max}$ [kN]	$F_{max}$	$F_{max}$	$\delta_p$ [mm]	$\delta_p$	$\delta_p$
		$F_{max,VB10}$	$F_{max,VE-15}$		$\delta_{p,VB10}$	$\delta_{p,VE-15}$
VB10	74.02	1.00	0.61	1.92	1.00	0.25
VBE-15	120.64	1.63	1.00	7.57	3.94	1.00
VBM-8	111.14	1.50	0.92	4.18	2.18	0.55
VBCB-10	131.22	1.77	1.09	6.37	3.32	0.84
VBCI-15	120.44	1.63	1.00	4.21	2.19	0.56

Table VIII : Main results obtained in the series of beams failing in shear

A more extensive research about the effectiveness of EBR and NSM techniques for increasing the shear resistance of RC beams can be found elsewhere [31].

## 7. Bond behaviour

### 7.1. Specimen configuration and test set up

The pullout-bending test is schematically represented in Fig. 14. The specimen is composed of

two blocks: block B where the CFRP is fixed to concrete along a bonded length of 325 mm; block A where the CFRP is bonded to concrete using distinct bond lengths (test region). This configuration assures that the bond failure will occur in block A.

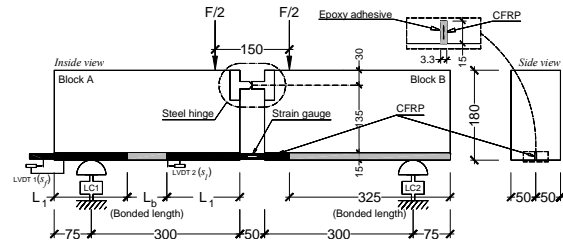


Fig. 14 : Specimen of the pullout-bending test

The slit where the CFRP is inserted had a 15 mm depth and a 3.3 mm width (see Fig. 14). The displacement transducer LVDT2 was used to control the test, at 5  $\mu\text{m/s}$ , and to measure the slip at the loaded end,  $s_l$ , while LVDT1 records the slip at the free end,  $s_f$ . The strain gauge glued to the CFRP at the symmetry axis of the specimen was used to estimate the pullout force on the CFRP at the loaded end. The applied forces were measured using two load cells (LC1 and LC2) placed at the supports of the specimen. The characteristics of the displacement transducers, strain gauge and load cells are described elsewhere [27]. Bond lengths of 40, 60 and 80 mm were considered for assessing its influence on bond behavior. To appraise the influence of concrete quality on CFRP bond behavior, three concrete mixes were designed with the average compression strength of 35 MPa, 45 MPa and 70 MPa. The experimental program, therefore, consisted of nine series, each one composed of three specimens. A generic series has the designation of fcmXX\_LbYY, where XX represents the concrete compression strength class, in MPa, and YY the CFRP bond length, in millimeters. The specimen preparation is described in detail elsewhere [32].

## 7.2. Results

### 7.2.1 Pullout Force versus Slip

Fig. 15 depicts the relationship between the pullout force and the slip at the loaded end for the series of distinct concrete strength classes. Each curve is the average response of three specimens. As is expected, the pullout force increased with the bond length,  $L_b$ . Since epoxy adhesive has a remarkably nonlinear behavior [25] and its volume increases with  $L_b$ , the nonlinear branch before peak pullout force also increased with  $L_b$ . As Tab. IX reveals, the influence of the concrete strength is marginal, especially in the maximum pullout force,  $F_{l,max}$ .

### 7.2.2 Bond Stress Versus Slip

Bond stress is obtained through dividing the pullout force by the contact area between CFRP and epoxy adhesive,  $F_l / (2(w_f + t_f)L_b)$ , where  $F_l$  is the pullout force, and  $w_f$  and  $t_f$  are the width and the thickness of the CFRP. Fig. 16 illustrates the relationship between the bond stress and the slip at the loaded end for the series of distinct bond lengths. Peak bond stress,  $\tau_{\max}$ , decreases with bond length and is practically insensitive to concrete strength, (see Tab. IX).

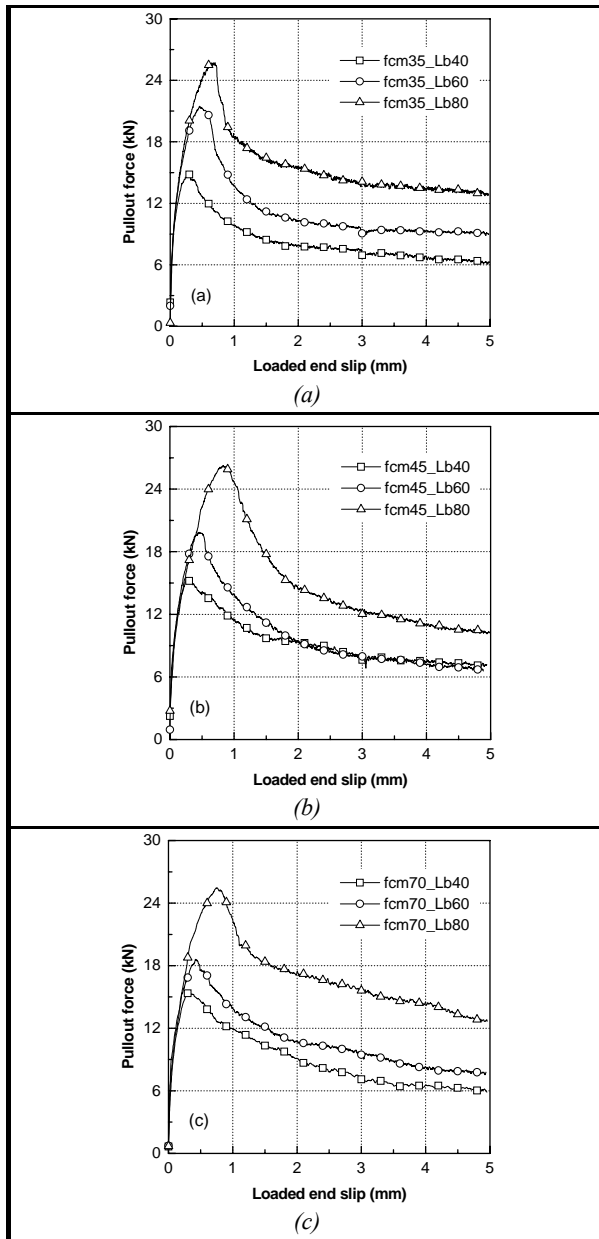


Fig. 15 : Pullout force-loaded end slip relationship for series of 35 MPa (a), 45 MPa (b) and 70 MPa (c) concrete compression strength classes

### 7.2.3 CFRP Stress at Peak Pullout Force

The influences of bond length and concrete strength on the stress of CFRP at peak pullout force,  $\sigma_{l\max}$ , are represented in Figs. 17 (a) and (b), respectively, where  $\sigma_{l\max}$  is normalized by the CFRP tensile strength,  $f_{fu} = 2740 \text{ MPa}$ . This influence can also be assessed from the results included in Tab. IX. Fig. 17 reveals that, in general,  $\sigma_{l\max} / f_{fu}$  increases with the bond length and is independent of the concrete strength.

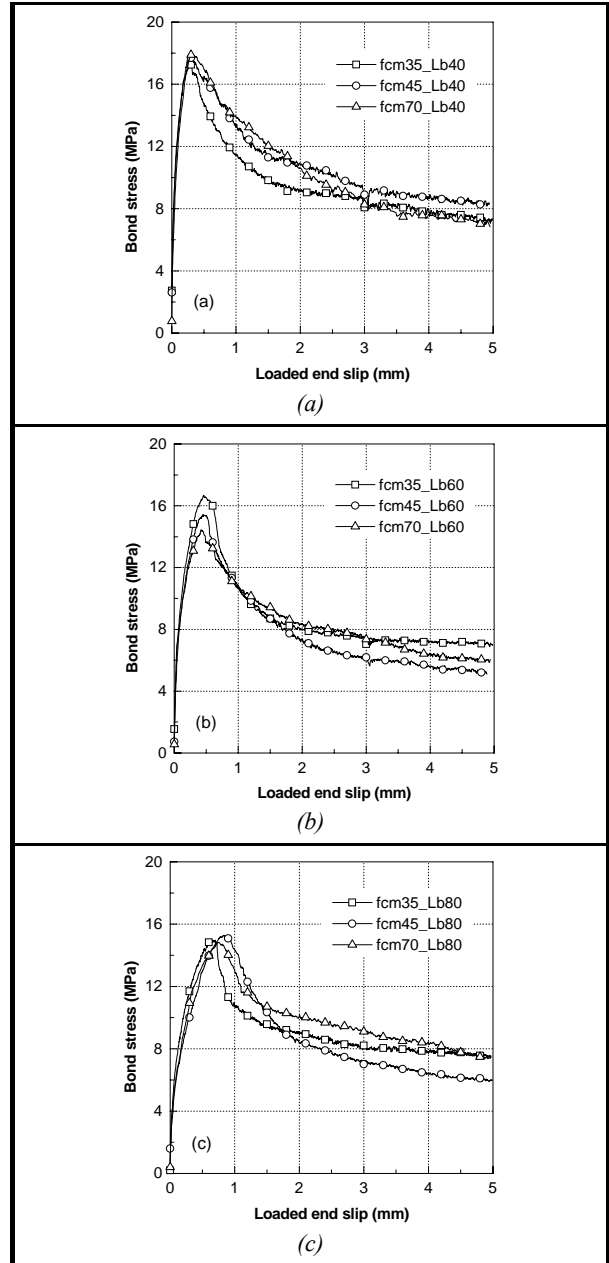


Fig. 16 : Bond stress-slip relationship for series of 40 mm (a), 60 mm (b) and 80 mm (c) bond lengths

### 7.2.4 Loaded End Slip at Peak Pullout Force

The influences of bond length and concrete strength on the loaded end slip at peak pullout force,  $s_{l\max}$ , are represented in Figs. 18 (a) and (b), respectively. A linear increasing trend of  $s_{l\max}$  with the bond length is observed in Fig. 18 (a), while an independence of the  $s_{l\max}$  on the concrete strength is shown in Fig. 18 (b) (see Tab. IX).

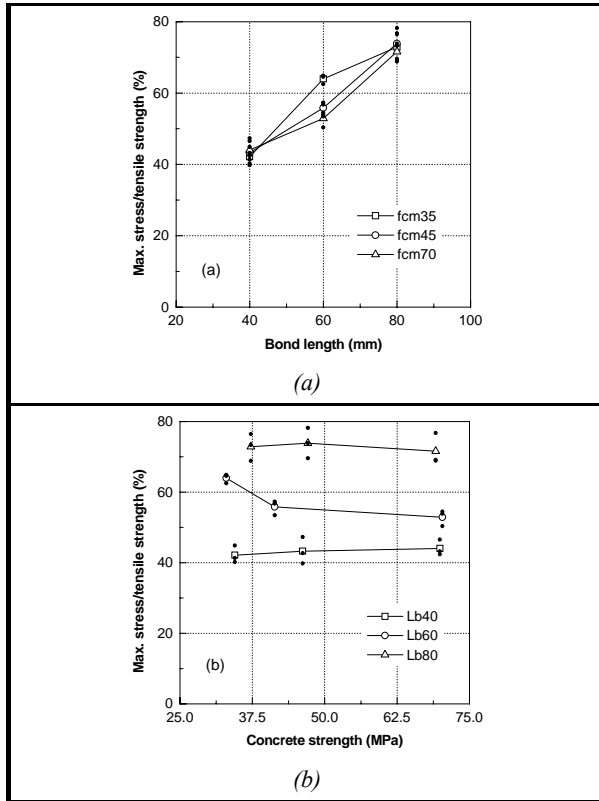


Fig. 17 : Influences of bond length (a) and concrete strength (b) on the tensile ratio  $\sigma_{l\max}/f_{fu}$

Series (1)	$F_{l\max}$ (kN) (2)	$\tau_{\max}$ (MPa) (3)	$\sigma_{l\max}/f_{fu}$ (%) (4)	$s_{l\max}$ (mm) (5)
fcm35_Lb40	15.0 (5.8%)	17.5	42.1	0.29 (21.5%)
fcm35_Lb60	15.5 (2.0%)	18.1	43.5	0.27 (26.8%)
fcm35_Lb80	15.7 (8.8%)	18.3	44.0	0.32 (10.5%)
fcm45_Lb40	22.8 (8.7%)	17.7	64.0	0.49 (5.8%)
fcm45_Lb60	19.9 (3.7%)	15.5	55.8	0.46 (8.8%)
fcm45_Lb80	18.9 (5.8%)	14.7	52.9	0.40 (10.0%)
fcm70_Lb40	22.4 (5.0%)	13.0	62.1	0.65 (16.0%)
fcm70_Lb60	26.4 (4.2%)	15.4	73.9	0.84 (30.6%)
fcm70_Lb80	25.6 (6.2%)	14.9	71.6	0.74 (3.0%)

Table IX : Average values of the main parameters evaluated

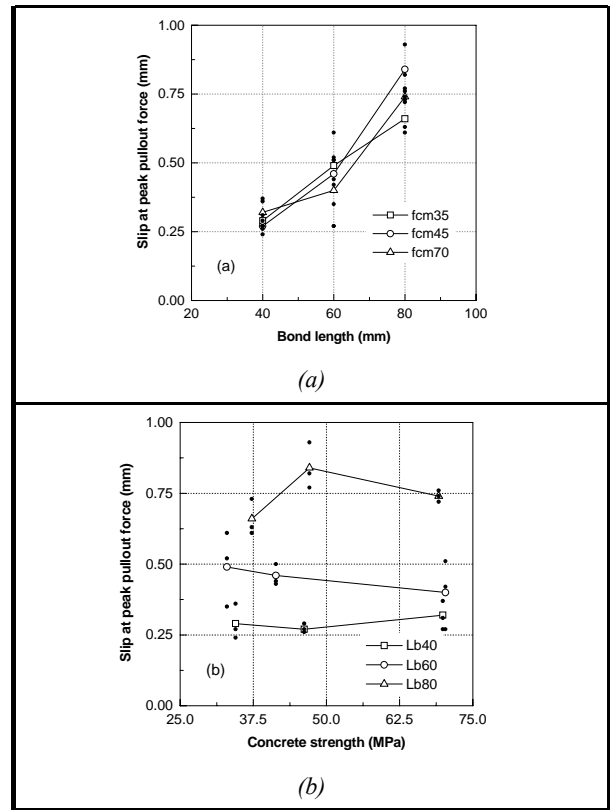


Fig. 18 : Influences of bond length (a) and concrete strength (b) on the loaded end slip at peak pullout force

## 8. Summary and Conclusions

To appraise the effectiveness of a Near Surface Mounted (NSM) strengthening technique for elements failing in bending and elements failing in shear, series of tests with concrete columns, concrete beams and masonry panels were carried out. The NSM technique was based on bonding laminate strips of Carbon Fiber Reinforced Polymer (CFRP) into grooves made onto the concrete cover of the elements to be strengthened. Data obtained from the carried out tests point out the following main observations.

### Concrete columns failing in bending

A CFRP cross sectional area,  $A_f$ , of 0.2% of the column cross sectional area,  $A_c$ , provided an average increase of 92% and 34% on the load carrying capacity of columns reinforced with 4 $\phi$ 10 and 4 $\phi$ 12 longitudinal steel bars (cross sectional area,  $A_s$ , of 314 mm<sup>2</sup> and 452 mm<sup>2</sup>, respectively, corresponding to a reinforcement ratio,  $\rho_s = A_s / A_c$ , of 0.79% and 1.13%). The premature debonding, generally occurring in the externally bonded reinforcing (EBR) technique, was avoided and strain values close to the CFRP ultimate rupture strain were measured on this

composite material. Some CFRP laminates have even failed at the failure crack of the concrete column. These results indicate that the strengthening technique proposed is very promising for increasing the load carrying capacity of concrete columns failing in bending.

### Concrete beams failing in bending

This strengthening technique was used for doubling the load carrying capacity of concrete beams failing in bending. This purpose was practically attained since an average increase of 91% on the maximum load was obtained. In addition, high deformability at the failure of the strengthened beams was assured. The NSM technique provided an average increase of: 51% on the load corresponding to concrete cracking; 32% on the load corresponding to the deflection of the serviceability limit state analysis and 28% on the rigidity at this load level, which are important benefits for design purposes; and 39% on the load at the onset of yielding the steel reinforcement. Maximum strain values ranging from 62% to 91% of the CFRP ultimate rupture strain were registered, revealing that this technique can mobilize stress levels close to the tensile strength of this composite material.

### Concrete beams failing in shear

The performance of EBR and NSM techniques on increasing the shear resistance of concrete beams failing in shear was compared. The NSM technique was based on bonding laminate strips of CFRP onto slits pre-cut onto the concrete cover of the vertical beam faces, which proved to be the most effective. The maximum load and the corresponding deflection of the beam strengthened with this technique were 9% larger and 16% smaller than the comparable values registered in the beam reinforced with steel stirrups of the equivalent shear reinforcement ratio. Beyond these structural benefits, it was verified that this technique was easier and faster to apply than the one based on embracing the beam with strips of CFRP sheet, which is a technique currently used for shear strengthening of concrete beams.

### Pullout bending tests

From the results obtained in the pullout bending tests, the following conclusions can be pointed out:

- The nonlinear branch before peak pullout force increased with  $L_b$ ;
- The peak pullout force increased with  $L_b$ ;
- The influence of the concrete strength on the pullout behavior was marginal;
- The bond strength ranged from 13 MPa to 18 MPa, revealed a tendency to decrease with the

increase of  $L_b$  and was practically insensitive to concrete strength;

- The ratio between the maximum tensile stress recorded on CFRP and its tensile strength increased with  $L_b$  and was independent of concrete strength;
- The loaded end slip at peak pullout force revealed a linear increasing trend with  $L_b$  and an independence of concrete strength.

## Acknowledgements

The authors of the present work wish to acknowledge the support provided by the S&P®, Bettor MBT® Portugal, Secil, Nordesfer, Ferseque, Casais, Solusel, VSL, Unibetão (Braga) and the collaboration of Cemacom.

## References

- [1] ACI Committee 440. Guide for the design and construction of externally bonded FRP systems for strengthening concrete structures. ACI, Technical report, May 2002, 118 pp.
- [2] CEB-FIB. Externally bonded FRP reinforcement for RC structures. International Federation for Structural Concrete – Technical report, July, 2001, 130 pp.
- [3] Nguyen DM, Chan TK, Cheong HK. Brittle failure and bond development length of CFRP-Concrete beams. *Journal of Composites for Construction*, February 2001, 5(1), 12-17.
- [4] Mukhopadhyaya P, Swamy RN. Interface shear stress: a new design criterion for plate debonding. *Journal of Composites for Construction*, February 2001, 5(1), 35-43.
- [5] Toutanji H, Balaguru P. Durability characteristics of concrete columns wrapped with FRP tow sheets. *Journal of Materials in Civil Engineering*, ASCE, 1998, 10(1), 52-57.
- [6] Pantuso A, Neubauer U, Rostasy FS. Effects of thermal mismatch between FRP and concrete on bond. In *Minutes of 4th ConcreteFibreCrete Meeting*, Lille, France, 2000.
- [7] De Lorenzis L, Nanni A, La Tegola A. Strengthening of reinforced concrete structures with near surface mounted FRP rods. *International Meeting on Composite Materials*, PLAST, Milan, Italy, May 2000, 8 pp.
- [8] Alkhrdaji T, Nanni A, Chen G, Barker M. Upgrading the transportation infrastructure: solid RD decks strengthened with FRP. *ACI Concrete International Journal*, 1999, 21(10), 37-41.
- [9] Hogue T, Cornforth RC, Nanni A. Myriad convention center floor system reinforcement. *Proceedings of the FRPRCS-4*, C.W. Dolan, S. Rizkalla and A. Nanni Editors, ACI, 1999, 1145-1161.
- [10] Tumialan JG, Galati N, Nanni A, Tyler D. Flexural strengthening of masonry walls in a high school using FRP bars. *Field Application of FRP Reinforcement*:

- Case Studies, ACI International SP-215, Eds. S. Rizkalla and A. Nanni, 2003, 413-428.
- [11] Blaschko M, Zilch K. Rehabilitation of concrete structures with CFRP strips glued into slits. Proceedings of the Twelfth International Conference of Composite Materials, ICCM 12, Paris, France, 1999.
- [12] Priestley MJN, Seible F. Design of seismic retrofit measures for concrete and masonry structures. Construction and Building Materials, 1995, 9(6), 365-377.
- [13] Xiao Y, Wu H. Compressive behavior of concrete confined by carbon fiber composite jackets. Journal of Materials in Civil Engineering, 2000, 12(2), 139-146.
- [14] Meier U. Bridge repair with high performance composites materials. Mater. Tech., Vol. 4, 1987, 125-128.
- [15] Untiveros C. Estudio Experimental del comportamiento del hormigón confinado sometido a compresión. PhD Thesis, UPC, Barcelona, Spain, 2000. (in Spanish)
- [16] Mirmiran A, Shahawy M, Samaan M, Echary HE, Mastrapa JC, Pico O. Effect of column parameters on FRP - confined concrete. Journal of Composites for Construction, 1998, 2(4), 175-185.
- [17] Taerwe L, Khalil H, Matthys S. Behaviour of RC beams strengthened in shear by external CFRP sheets. Proceedings of the Third International Symposium Non-Metallic (FRP) Reinforcement for Concrete Structures, Vol. 1, Tokyo, October 1997, 483-490.
- [18] Chaallal O, Nollet MJ, Perraton D. Renforcement au cisaillement de poutres en béton armé par des lamelles composites collées à laide de résine époxy. Bulletin des Laboratoires des Ponts et Chaussees - 212, Novembre/Decembre 1997, 87-93.
- [19] Triantafillou T. Shear strengthening of reinforced concrete beams using epoxy-bonded FRP composites. ACI Structural Journal, March-April 1998, 107-115.
- [20] De Lorenzis L, Nanni A, La Tegola A. Flexural and shear strengthening of reinforced concrete structures with near surface mounted FRP rods. Proceedings of the Third International Conference on Advanced Composite Materials in Bridges and Structures, Ottawa, Canada, Editors: J. Humar and A.G. Razaqpur, August 2000, 521-528.
- [21] RILEM (1982). "Bond test for reinforcement stell. 1. Beam test.", TC9-RC.
- [22] RILEM Draft Recommendation, 50-FMC Committee Fracture Mechanics of Concrete. Determination of the fracture energy of mortar and concrete by means of three-point bending tests on notched beams. Materials and Structures, 1985, 85(85), 285-290.
- [23] EN 10 002-1. Metallic materials. Tensile testing. Part 1: Method of test (at ambient temperature). 1990, 35 pp.
- [24] ISO 527-5. Plastics - Determination of tensile properties - Part 5: Test conditions for unidirectional fibre-reinforced plastic composites. International Organization for Standardization, Genève, Switzerland, 1997, 9 pp.
- [25] Sena-Cruz JM, Barros JAO, Faria RMCM. Assessing the embedded length of epoxy-bonded carbon laminates by pull-out bending tests. International Conference Composites in Construction, Porto, Portugal, October 2001, 217-222.
- [26] Sena-Cruz JM, Barros JAO. Bond behavior of carbon laminate strips into concrete by pullout-bending tests. Bond in Concrete - from the research to standards, International Symposium, November 2002, Budapest, Hungary, 614-621.
- [27] ISO 527-3. Plastics - Determination of tensile properties - Part 5: Test conditions for unidirectional fibre-reinforced plastic composites. International Organization for Standardization, Genève, Switzerland, 1997, 5 pp.
- [28] EN 196-1. Methods of testing cement. Part 1: Determination of strength. 1996, 26 pp.
- [29] Ferreira DRSM. Pilares de Betão Armado Reforçados com Laminados de Fibras de Carbono (Reinforced concrete columns strengthened with CFRP laminates). MSc Thesis, Civil Eng. Dep., University of Minho, Portugal, 2000. (in Portuguese)
- [30] Barros, J.A.O., Fortes, A.S., "Flexural strengthening of concrete beams with CFRP laminates bonded into slits", accepted to be published in the Cement and Concrete Composites Journal.
- [31] Dias, S.J.E.; Barros, J.A.O., "CFRP no reforço ao corte de vigas de BA: investigação experimental e modelos analíticos", Technical report 04-DEC/E-08, Dep. Civil Eng., University of Minho, 109 pp, Maio 2004. (in Portuguese)
- [32] Sena-Cruz, J.M.; Barros, J.A.O., "Bond between near-surface mounted CFRP laminate strips and concrete in structural strengthening", accepted to be published in the Composites for Construction Journal, 2004.